Mismatch repair-dependent transcriptome changes in human cells treated with the methylating agent N-methyl-n'-nitro-N-nitrosoguanidine

di Pietro, M ; Marra, Giancarlo ; Cejka, P ; Stojic, L ; Menigatti, M ; Cattaruzza, M S ; Jiricny, J

Abstract: DNA mismatch repair (MMR) plays a key role in the cytotoxic response of human cells to methylating agents, however, the cascade of events leading to cell cycle arrest and cell death has yet to be characterized. We studied the role of MMR in the transcriptional response to DNA methylation damage in two human cellular models: (a). the lymphoblastoid cell line TK6 and its derivative MT1, which is mutated in the MMR gene hMSH6; and (b). the epithelial cell line 293T Lalpha in which the expression of the MMR gene hMLH1 can be tightly regulated and p53 is inactivated. Upon N-methyl-N'-nitro-N-nitrosoguanidine treatment, only cells with functional MMR were killed, but the type of cytotoxic response differed. In TK6 cells, S-phase arrest and apoptosis were accompanied by a dramatic change in gene expression, notably, an up-regulation of several genes encoding growth inhibitors and proapoptotic factors both p53 dependent and independent. In contrast, the MMR-dependent transcriptional response in 293T Lalpha cells was substantially less pronounced than in TK6 cells, despite an efficient induction of a G(2)-M checkpoint and nonapoptotic cell death. Thus, we demonstrate that in human cells of different origin, MMR-mediated killing by methylating agents occurs through different pathways and regardless of the p53 status. Moreover, once DNA methylation damage has been processed by the MMR system, tumor cells might be committed to die, although one or more of their signaling pathways are impaired.

[CANCER RESEARCH 63, 8158–8166, December 1, 2003]

Mismatch Repair-Dependent Transcriptome Changes In Human Cells Treated with the Methylating Agent *N*-Methyl-*N*′-Nitro-*N*-Nitrosoguanidine

Massimiliano di Pietro,[1] Giancarlo Marra,[1] Petr Cejka,[1] Lovorka Stojic,[1] Mirco Menigatti,[1] Maria Sofia Cattaruzza,[2] and Josef Jiricny[1]

[1]Institute of Molecular Cancer Research, University of Zurich, Zurich, Switzerland, and [2]Department of Public Health, University "La Sapienza," Rome, Italy

ABSTRACT

DNA mismatch repair (MMR) plays a key role in the cytotoxic response of human cells to methylating agents, however, the cascade of events leading to cell cycle arrest and cell death has yet to be characterized. We studied the role of MMR in the transcriptional response to DNA methylation damage in two human cellular models: (*a*) the lymphoblastoid cell line TK6 and its derivative MT1, which is mutated in the MMR gene *hMSH6*; and (*b*) the epithelial cell line 293T Lα in which the expression of the MMR gene *hMLH1* can be tightly regulated and p53 is inactivated. Upon *N*-methyl-*N*′-nitro-*N*-nitrosoguanidine treatment, only cells with functional MMR were killed, but the type of cytotoxic response differed. In TK6 cells, S-phase arrest and apoptosis were accompanied by a dramatic change in gene expression, notably, an up-regulation of several genes encoding growth inhibitors and proapoptotic factors both p53 dependent and independent. In contrast, the MMR-dependent transcriptional response in 293T Lα cells was substantially less pronounced than in TK6 cells, despite an efficient induction of a G_2-M checkpoint and nonapoptotic cell death. Thus, we demonstrate that in human cells of different origin, MMR-mediated killing by methylating agents occurs through different pathways and regardless of the p53 status. Moreover, once DNA methylation damage has been processed by the MMR system, tumor cells might be committed to die, although one or more of their signaling pathways are impaired.

INTRODUCTION

Alkylating agents were introduced into clinical practice > 50 years ago when their antitumor properties, linked to their ability to covalently modify nucleophilic centers in DNA, were demonstrated. A subgroup of these agents, mainly hydrazine and triazine derivatives MNNG,[3] *N*-methyl-*N*-nitrosourea, and temozolomide, have one reactive group and react with only one strand of DNA. The reaction primarily associated with the mutagenicity of these agents is the methylation of the O^6 position of guanines in DNA. When the methyl group is not removed by the detoxifying enzyme MGMT, O^6-methylguanine can mispair with thymine during DNA replication, which results in G/C to A/T transitions. Paradoxically, the cytotoxicity of methylating agents has been attributed to the antimutagenic attempts of the MMR system to process these O^6-meG/T mismatches, the hypothesis being that mismatch correction directed to the newly synthesized strand (carrying the thymine) would be ineffectual as long as the methylated base in the template strand persists. Reiterated cycles of MMR-driven exonucleolytic degradation of the newly synthesized strand, followed by DNA synthesis and reintroduction of T opposite to O^6-meG, are presumed to result in cell cycle arrest and lethality (1). Whether this hypothesis is correct, a characteristic phenotype of the MMR-deficient human cells, *i.e.,* tolerance to monofunctional methylating agents, corroborates a relationship between methylation-induced killing and repair attempts. This phenotype was first described in 1993 in two seminal works in which *N*-methyl-*N*-nitrosourea-tolerant human and rodent cell lines were found to be defective in DNA mismatch binding (2), and the MMR-deficient human lymphoblastoid MT1 cell line showed G/C to A/T transitions in the *HPRT* gene upon MNNG treatment (3). Consistent with these findings, the sensitivity to MNNG in the MMR-deficient human colon cancer cell line HCT116 (mutated in both alleles of the MMR gene *hMLH1*) was restored by expression of a functional *hMLH1* gene in a chromosome transfer experiment (4, 5). A series of studies followed in which the methylation-tolerance phenotype was confirmed in all human and rodent cells with impaired MMR, regardless of the MMR gene mutated (*hMSH2*, *hMSH6*, *hMLH1*, or *hPMS2*; Ref. 6). The relationship between MMR deficiency and tolerance to methylating agents could recently be verified in a truly isogenic cellular model, the 293T Lα cell line established in our laboratory in which the expression of hMLH1 can be tightly regulated (7).

The clinical implications of these studies are that tumors with nonfunctional MMR (~15% of colon cancers) should not be responsive to deployment of methylating agents, and MMR-deficient cells in a tumor might be selected for during such treatment (6). The other known causes of reduced cellular sensitivity to methylating agents are typical resistance mechanisms acting upstream of O^6-meG/T mispairing, one being the overexpression of MGMT. This enzyme plays an important role in DNA detoxification by removing methyl- and other small alkyl groups from the O^6 position of guanine. Thus, tumors with functional MMR and low levels of MGMT should respond favorably to methylating agents. This situation arises rather frequently because the levels of MGMT vary widely among individuals. Moreover, the *MGMT* gene was shown to be silenced by promoter methylation in many tumor types, *i.e.,* in ~40% of MMR-proficient colorectal cancers (8). However, as the sensitivity to methylating agents ultimately depends on the processing of the damage by MMR, it is crucial to identify the cascade of events that is triggered by this repair process and that ultimately leads to cell death. To date, it has been demonstrated that p53 is stabilized and apoptosis is induced in the MMR-proficient lymphoblastoid cell line TK6 (9), that MNNG-induced apoptosis depends on the function of the hMSH2/hMSH6 mismatch recognition heterodimer and occurs also in TK6 cells in the absence of p53 (10), and that p53 phosphorylation on serine residues 15 and 392 is dependent on the presence of functional hMSH2/hMSH6 and hMLH1/hPMS2 complexes (11). To gain more insight into the MMR-mediated cytotoxicity of methylating agents, we investigated the global transcriptional response to MNNG in cell lines harboring diverse combinations of MMR- and p53 status, all devoid of MGMT.

MATERIALS AND METHODS

Cell Lines. The human B lymphoblastoid cell lines TK6 and MT1 were a gift of William G. Thilly (Massachusetts Institute of Technology, Cambridge, MA), and WTK1 was kindly provided by Phaik Morgenthaler (University of

Received 5/29/03; revised 9/17/03; accepted 9/30/03.

Grant support: Swiss National Science Foundation (to M. d. P., J. J.), the Union Bank of Switzerland (to P. C.) and the European Community (to L. S.).

The costs of publication of this article were defrayed in part by the payment of page charges. This article must therefore be hereby marked *advertisement* in accordance with 18 U.S.C. Section 1734 solely to indicate this fact.

Requests for reprints: Giancarlo Marra, Phone: 41-1-634-8927; Fax: 41-1-634-8904; E-mail: marra@imr.unizh.ch.

[3] The abbreviations used are: MNNG, *N*-methyl-N′-nitro-*N*-nitrosoguanidine; MGMT, methylguanine methyl transferase; MMR, mismatch repair; O^6-meG/T, O^6-methylG/T; TBE, Tris-borate/EDTA; EL, experimental line; BL, base line; RT-PCR, reverse transcription-PCR; TAC, threshold amplification cycle; GAPDH, glyceraldehyde-3-phosphate dehydrogenase; PARP, poly(ADP-ribose) polymerase; TGF, tumor growth factor.

Lausanne, Lausanne, Switzerland). These cells were cultured at 37°C in a 5% CO_2 humidified atmosphere and maintained in RPMI 1640 supplemented with 10% FCS and 2 mM L-glutamine (Life Technologies, Inc.). The cell line 293T Lα^+/Lα^- was recently developed in our laboratory (7) from HEK293T human embryonic kidney cells, immortalized with adenovirus 5 DNA, and additionally transfected with large T antigen from SV40 (12). The *hMLH1* gene in this line is epigenetically silenced by promoter hypermethylation (13). *hMLH1* cDNA was stably introduced into this line under the control of the tetracycline response promoter, using the Tet-Off system (Clontech). In the absence of doxycycline, this cell line expresses the wild-type hMLH1 protein and is MMR proficient (293T Lα^+), whereas the addition of doxycycline specifically turns off hMLH1 expression (293T Lα^-) and brings about MMR deficiency. These cells were cultured at 37°C in a 5% CO_2-humidified atmosphere and maintained in DMEM (Life Technologies, Inc.) supplemented with 10% tetracycline-free FCS (Clontech), 2 mM L-glutamine, 300 μg/ml hygromycin B (Roche), 100 μg/ml Zeocin (Invitrogen), and 50 ng/ml doxycycline when necessary (Clontech).

Cell Cycle Analysis. A total of 1.2×10^6 cells was washed with PBS and fixed in ice-cold 70% ethanol. They were treated with 200 units/ml RNase A and stained with 20 μg/ml propidium iodide. Cell cycle analysis was performed using a Becton Dickinson FACscan flow cytometer and Cell Quest software.

Pulse Field Gel Electrophoresis. Cells were washed and mixed with low melting agarose at 43°C. Agarose plugs were incubated overnight at 50°C with gentle agitation in lysis buffer [100 mM EDTA (pH 8), 10 mM Tris-HCl (pH 8.0), 1% sarcosyl, and 100 μg/ml proteinase K] followed by a second overnight incubation at 37°C with fresh lysis buffer. After equilibration in TBE buffer, the agarose plugs were loaded in the wells of 1% pulse field-certified agarose (Bio-Rad) in TBE buffer. Electrophoresis was carried out in the CHEF-DR III Pulse Field Electrophoresis System (Bio-Rad) as follows: 14°C, switch time 50–90 s, run time 22 h, angle 120°, and voltage gradient 6 V/cm. Finally, the DNA was stained with ethidium bromide in TBE buffer.

Microscopy. Cells were plated on coverslips in 6-well culture plates and exposed to MNNG at 37°C in a 5% CO_2-humidified atmosphere. After fixation with 3.7% formaldehyde/PBS for 15 min at 4°C and washing with PBS, 4′,6′-diamidino-2-phenylindole hydrochloride (Sigma) was added (0.1 μg/ml) for 30 min at 37°C. Finally, the coverslips were mounted in 50% glycerol, and DNA morphology was examined by fluorescence microscopy (Leica DC 200).

Microarray Experiments. Total RNA was isolated from 5×10^6 TK6, MT1, or WTK1 cells, untreated or 30 h after treatment with 0.4 μM MNNG or from 7×10^6 293T Lα^+ or Lα^- cells, untreated, or 12, 30, and 72 h after 0.2 μM MNNG treatment, using an affinity resin column (RNeasy; Qiagen). Total RNA was converted to cDNA using a cDNA synthesis kit (Invitrogen). Double-stranded cDNA was then converted to biotin-labeled cRNA by a T7 RNA polymerase-catalyzed reaction (MEGA Script; Ambion) with biotin-containing ribonucleotides (LOXO). Labeled cRNAs were then purified (RNeasy; Qiagen) and fragmented. Fifteen μg of cRNA were used to hybridize with Affymetrix U95Av2 chips (Affymetrix) carrying *in situ* synthesized oligonucleotides representing >12,000 functionally characterized sequences.

Data Analysis. Expression profiles were analyzed in three independent experiments using the Data Mining Tool software (Affymetrix). For each comparison, three ELs, *e.g.,* treated cells, were compared with three BLs, *e.g.,* untreated cells. Data were evaluated with both the absolute analysis and the comparative analysis algorithms. The former algorithm measures, for each array, the abundance of transcripts (signal) and the specificity of hybridization (P = present, M = marginally present, A = absent). The latter algorithm compares two arrays (one EL *versus* one BL, *e.g.,* nine comparisons for three arrays/group) and indicates, for each gene, the direction of the change (I = increased, MI = moderately increased, NC = not changed, MD = moderately decreased, D = decreased).

To eliminate genes with low abundance and specificity of hybridization and to identify significant changes, we used a two-step selection procedure. For TK6 and MT1 cells in which only one time point after treatment was evaluated, in the first step, we compared three ELs *versus* three BLs and selected genes matching all of the following four criteria: (*a*) at least one P or M of the 6 arrays; (*b*) signal > 50 in at least one of these arrays; (*c*) fold change >1.8 or <-1.8 (average signal of three ELs *versus* three BLs); and (*d*) Mann Whitney $P < 0.05$. In the second step, the selected genes were filtered using an arbitrary score system based on: (*a*) signal: average EL for up-regulated genes (or average BL for down-regulated) >1000, 1000 < 100, or <100 (points 2, 1, or 0, respectively); (*b*) number of "P + M": 3, 2, or 1 (points 2, 1, or 0, respectively) in the three ELs for up-regulated genes (or in the three BLs for down-regulated); (*c*) number of "I + MI" in nine comparisons (for up-regulation) or "D + MD" (for down-regulation): points 3 (from seven to nine times), 2 (from four to six), 1 (from one to three), and 0 (all NC). With a maximum of seven points, a score ≥ 4 was considered significant. The same procedure was applied in the comparison between untreated MT1 and TK6 where MT1 were considered the EL.

For 293T Lα cells in which four time points were analyzed (time point 0, untreated; time points 12, 30, and 72 h after treatment), the two-step selection procedure was applied to the following comparisons: 293T Lα^+ *versus* Lα^- at 0, 12, 30, and 72 h, and untreated *versus* treated (time point 0 *versus* each time point after treatment for both Lα^+ and Lα^-). Genes with score ≥ 4 were then analyzed with multiple linear regression to estimate the independent role of each of the explanatory variables (presence of MLH1 and time after treatment) on the change of the signal.

Quantitative RT-PCR. One-step RT-real time PCR was performed with the Roche LightCycler System using the Light Cycle-RNA Master Sybr Green I Kit (Roche) according to the manufacturer's instructions, 0.3 μM of each oligonucleotide primer (Microsynth) and 300 ng of total RNA in 20 μl of reaction volume. Primer sequences and RT-PCR reaction conditions are available on request. The cycle corresponding to the beginning of the log-phase amplification was denominated TAC. One cycle difference in TAC corresponds theoretically to a 2-fold change in RNA concentration. Fold changes were obtained by normalizing to GAPDH used as internal reference. All of the experiments were performed in duplicate, and the specificity of each amplification product was verified by agarose gel electrophoresis.

Western Blotting. Western blotting was performed as previously described (7) by using the following primary antibodies: TFIIHp89, Santa Cruz Biotechnology sc-293; β-tubulin, Santa Cruz Biotechnology sc-5274; p53, Santa Cruz Biotechnology sc-98; PIG3, Oncogene Research OP148; p21, 05-345 Upstate; c-myc, Santa Cruz Biotechnology sc-40; bcl-2, Transduction Laboratories 610538; XPC, kindly provided by Jan Hoeijmakers; PARP, Calbiochem AM30; hPMS2 PharMingen 556415; and hMLH1 PharMingen 554072.

RESULTS

The lymphoblastoid cell line MT1 was derived from TK6 cells by treatment with the Acridine ICR191 and selection for resistant clones with MNNG (14). MT1 cells are MMR deficient because both alleles of *hMSH6* carry different missense mutations (15). We exposed both cell lines to 0.4 μM MNNG (IC_{90} for TK6) and evaluated the cell cycle distribution by flow cytometry. TK6 cells accumulated in S phase as early as 24 h after treatment (Fig. 1*A*). The sub-G_1 peak observed at later time points, along with the presence of DNA fragmentation (Fig. 1*D*) and PARP cleavage (Fig. 1*E*), was indicative of apoptosis induction. In contrast, the cell cycle distribution was completely unaffected in MT1 cells (Fig. 1*A*).

RNA was isolated from TK6 and MT1 cells 30 h after treatment because at this time point the significant changes observed in cell cycle perturbation were expected to be accompanied by alterations in the transcriptome. In Fig. 2, the scatter graphs show an overview of the gene expression changes in TK6 (*A*) and MT1 (*B*) upon treatment. A dramatic change in the transcriptome of TK6 cells contrasted with the stability of RNA levels in MT1 cells. Applying the two-step selection procedure described in "Materials and Methods," we did not find statistically significant changes in MT1 cells, whereas 340 genes were up-regulated or down-regulated >1.8-fold in TK6 cells (Table A, supplementary material). A selection of these genes is listed in Table 1, categorized according to their putative function. In accordance with the cellular response observed, among up-regulated transcripts were the products of several proapoptotic genes (PIG3, PUMA, BAX, Fas/APO1, and TNFSF10), cell cycle regulators (p21/WAF1, GADD45, 14-3-3σ, SMAD5, SMAD3, and CDC6) and growth

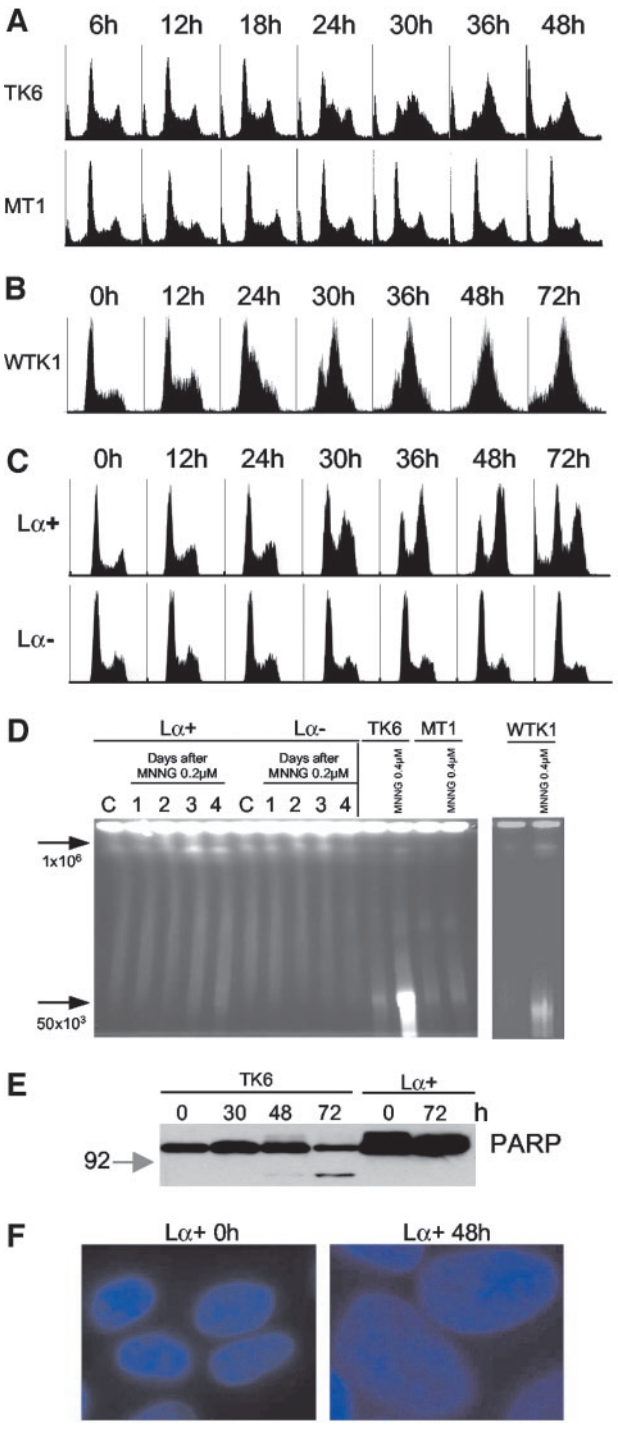

Fig. 1. Flow-cytometric analysis of cell cycle progression of TK6, MT1 (*A*), WTK1 (*B*), and 293T Lα^+/Lα^- (*C*) cells after treatment with MNNG. TK6 and WTK1 underwent an S-phase arrest, whereas 293T Lα^+ cells arrested in G_2-M. No alteration in cell cycle progression was observed in MT1 and 293T Lα^- cells. *D*, DNA fragmentation analysis by Pulse Field Gel Electrophoresis. Only TK6 and WTK1 cells showed DNA fragmentation (~50 kb) 72 h after MNNG treatment. *E*, Western blot showing cleavage of PARP to the characteristic M_r 89,000 fragment in TK6 cells 72 h after treatment. *F*, 4′,6′-diamidino-2-phenylindole hydrochloride staining of 293T Lα^+ cells 48 h after treatment, showing a substantial increase in nuclear size that is indicative of G_2-M arrest.

inhibitors (MIC-1, CEACAM1, BTG2, BTG1, and TIEG). The DNA repair genes XP-C, DDB2, RAD51 L3, ligase I, and BRCA2 were also up-regulated, along with several genes involved in metabolism, cytoskeleton organization, and transcription. As shown in Fig. 2*C*, we could verify the reliability of the microarray data by quantitative RT-PCR for all of the genes tested. Furthermore, most of the genes found differentially regulated in a previous study using subtractive hybridization and Northern blot (our unpublished results) were identified in this study.

In accordance with the increase of p53 protein in TK6 cells (Fig. 2*D*), we detected up-regulation of the transcripts of many p53-target genes (Table 1) and for some such as PIG3 and XP-C for which antibodies were available, an increase in protein levels was also observed (Fig. 2, *D* and *F*, respectively). Conversely, the protein level of the p53-target p21/WAF1 (Fig. 2*D*) was unchanged until 72 h after treatment, despite the early rise in RNA level. To investigate the role of p53 in the transcriptional response of lymphoblastoid cells to MNNG, we examined the MMR-proficient WTK1 cells, which were derived from the same progenitor as TK6 but harbor a homozygous missense mutation in the *p53* gene that leads to overexpression of an inactive form of the protein (16). Treatment of WTK1 cells arrested them in S phase and precipitated apoptosis, but the appearance of apoptotic cells was delayed by 24 h as compared with TK6 (Fig. 1, *B* and *D*), as reported earlier (10). Microarray analysis (Table 1, genes in bold, and Table C, supplementary material) showed a p53-independent up-regulation of several cell cycle regulators and proapoptotic factors in WTK1 cells (see "Discussion").

In TK6 cells, the most down-regulated gene was *c-myc*, a promoter of cell cycle progression (17), the protein level of which dramatically decreased (Fig. 2*E*), presumably via repression mediated by the TGF-β effectors SMADs (18). Among the other down-regulated genes were growth stimulators (IRF4, INSIG1 and INSR) and cell cycle modulators (DIM1 and cyclin B1), as well as transcripts of four heat shock proteins, which play a role in preventing apoptosis (19).

Because MT1 was derived from TK6, it was important to know to what extent the two cell lines could be considered isogenic. Comparison of their basal gene expression profiles (Fig. 2*I*) showed noticeable differences, and after the two-step selection procedure, we identified several significant changes (Table B, supplementary material) that might contribute to the absence of any detectable effect of MNNG on MT1. Among the overexpressed genes, we found the antiapoptotic factors CD44 (different isoforms increased between 10- and 44-fold) and Bcl-2 (confirmed at protein level in Fig. 2*G*), whereas some proapoptotic molecules (BNIP3L, CD20, DAPK1, caspase-6, and TNFRSF9) and growth inhibitors (GADD45 A and B, GAS-7) were underexpressed. In an attempt to test the integrity of the p53-dependent signaling, we treated MT1 cells with 23 μM MNNG (IC_{90} for this cell line). This dose efficiently induced p53 stabilization and transcription of its targets p21/WAF1, PIG3, and XP-C (Fig. 2, *F* and *H*).

These results prompted us to use the isogenic system consisting of the hMLH1-negative 293T cell line in which the expression of the stably transfected *hMLH1* gene can be induced by doxycycline withdrawal. In this cell line, p53 is inactivated, and the apoptotic response is likely to be impaired, as witnessed also by its extreme resistance to Fas ligand treatment (our unpublished results). To rule out secondary changes in the transcriptome induced by the overexpression of hMLH1, we compared the RNA population of 293T Lα^+ with that of Lα^- cells. The isogenicity of this cellular system was demonstrated by the very narrow distribution of the transcripts along the central diagonal line (Fig. 2*J*) and additionally confirmed by the absence of significant gene expression differences (*i.e.,* score ≥ 4) showed by the two-step-selection procedure, with the notable exception of hMLH1. Also, the exposure to doxycycline in the absence of the vector carrying hMLH1 did not induce any changes in transcript levels (Fig. 1, supplementary material).

The treatment of 293T Lα cells with 0.2 μM MNNG (IC_{90} for Lα^+) caused a perturbation in the cell cycle (Fig. 1*C*) and finally

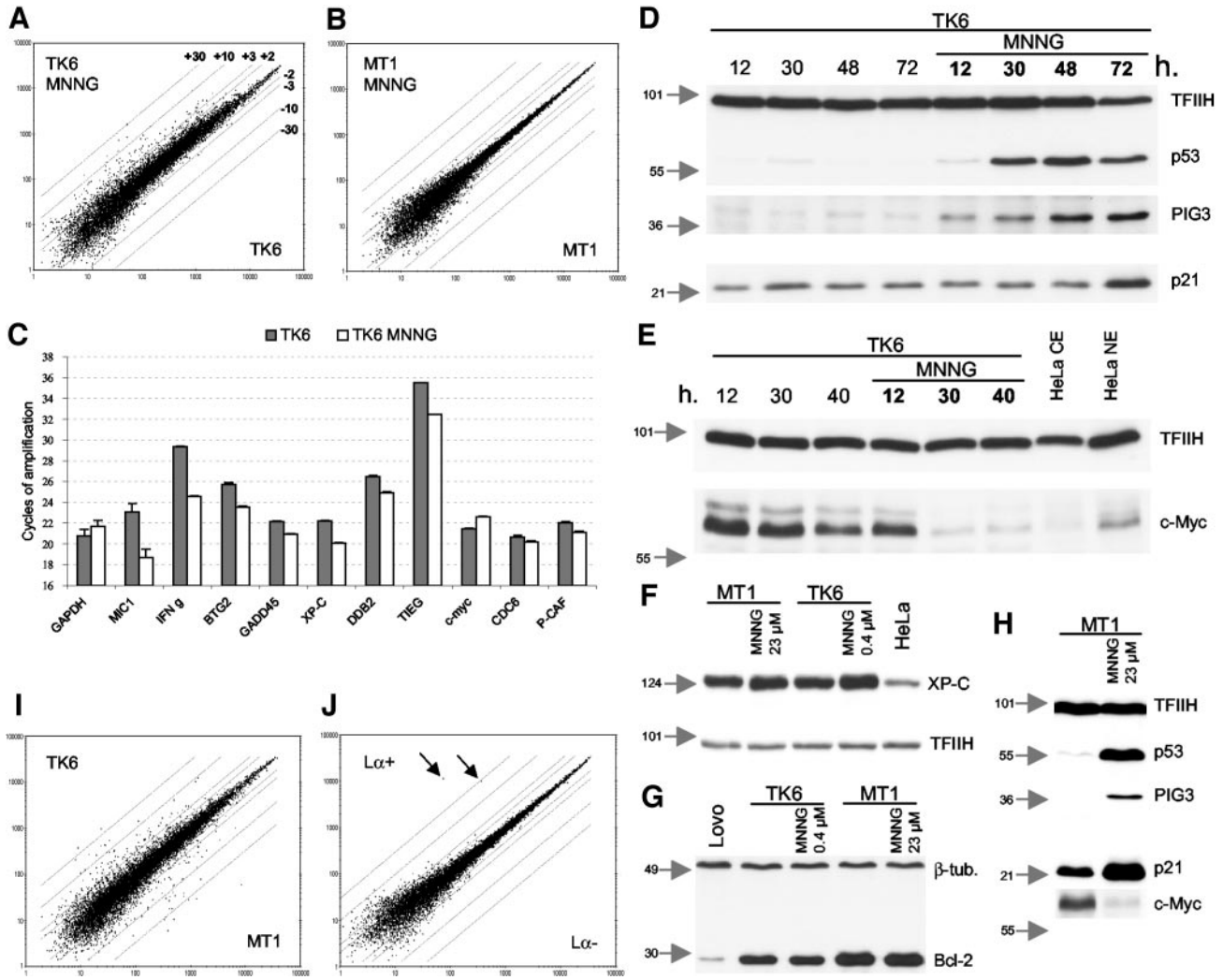

Fig. 2. Microarray data and quantitative evaluation of RNA and proteins in TK6 and MT1 cells. The scatter graphs show the overall changes of TK6 (*A*) and MT1 (*B*) transcriptomes upon MNNG treatment (x and y axes: *signal* values). Each dot represents a gene and the four diagonal lines correspond to different fold changes of expression (*i.e.,* dots outside the two inner lines represent transcripts the levels of which deviated >2-fold from the central line). Hundreds of dots spreading over the 2-fold change lines (*A*) indicate dramatic changes in gene modulation in the TK6 cells upon MNNG treatment. The transcriptome of MT1 cells (*B*) remained globally unmodified upon similar treatment. N.B., the *bottom left parts* of the graphs carry limited significance because transcripts of low abundance are difficult to quantitate reproducibly. *C*, quantitative analysis of transcripts by RT-PCR. The height of the *bars* corresponds to TAC (see "Materials and Methods") and inversely correlates with the abundance of the transcript (some *error bars* are very small and not visible in this picture). GAPDH was used as control. *D–H*, Western blot analyses (see "Results"). TFIIHp89 and β-tubulin: loading controls. *I* and *J*, scatter graphs obtained by comparing the basal level of transcripts in the MMR-proficient cells with the respective MMR-deficient counterparts. A substantial number of genes were differentially expressed in MT1 cells as compared with TK6 (*I*). No differences were detectable in 293T $L\alpha^+$ *versus* $L\alpha^-$ cells (*J*), except for the two hMLH1probes (*arrowed*).

cell death, albeit only in the presence of functional MMR, *i.e.,* in 293T $L\alpha^+$ cells. Accumulation of cells with a DNA content of 4n was observed as early as 30 h, and a sub-G_1 peak was evident after 48 h. As expected, nuclei of G_2-M arrested 293T $L\alpha^+$ cells appeared considerably larger than in untreated cells (Fig. 1*F*), but no apoptotic bodies were detectable at later time points. In addition, we failed to detect DNA fragmentation (Fig. 1*D*) and PARP cleavage (Fig. 1*E*).

Despite the dramatic impact of the presence of hMLH1 on the cellular fate in response to MNNG, we detected relatively few genes differentially transcribed in 293T $L\alpha^+$ cells compared with $L\alpha^-$ 30 h after treatment (Fig. 3*A*), as well as at other time points. In addition, MNNG treatment affected the transcriptome of 293T Lα cells regardless of the MMR status. By multiple regression analysis, we could distinguish gene regulations induced by the genotoxic treatment *per se* from changes after MMR-dependent DNA damage processing. As shown in Table 2, the genes belonging to the latter category (Table 2*A*) were not as numerous as those regulated upon MNNG treatment independently of the MMR status (Table 2*B*; complete list in Table D, supplementary material). Most of the significant changes between MMR-proficient and MMR-deficient cells were recorded at the latest time point (72 h). Indeed, at this time, we observed in 293T $L\alpha^+$ cells an augmented expression of genes encoding proteins involved in signaling such as the kinases SNK, FAK, and CLK1 and the growth inhibitors PTGER2 (20) and IGFBP7/Mac25 (Ref. 21; Table 2*A*). The increased level of IGFBP7/Mac25 mRNA was confirmed by RT-PCR (Fig. 3*B*).

The majority of changes induced by MNNG independently of the MMR status were present already 12 h after treatment. A paradigm is the transcription factor ATF3 that has been reported to be transcriptionally induced upon DNA damage (22). ATF3 was up-regulated in 293T Lα cells to the same extent as in TK6 and MT1 (the latter treated with an equitoxic concentration of MNNG; Fig. 3*C*). Thus, 293T cells are likely to sense the MNNG treatment also in the absence of MMR, as further witnessed by the up-regulation of the two stress response factors STK39 and GADD34. As p53 is stabilized and inactivated in

Table 1 *A selection of the 340 transcripts that significantly changed in TK6 cells upon MNNG treatment*

Genes in bold were found up-regulated also in treated WTK1 cells (complete lists in Tables A and C of supplementary material).

Category[a]	GeneBank access. no.	Title	Function[a]	Fold change[b]	Score[c]
Up-regulated genes					
Metabolism	M29877	**L-fucosidase α**	Glycan metabolism	30.8	7
	J03826	Ferrodoxin reductase	Electron transport	3.5	7
	M30474	γGT2	Amino acid metabolism	3.0	7
Cytoskeleton	AF001691	Periplakin	Cell shape control	20.2	6
	X13839	Vascular smooth α actin	Cell shape control	4.6	7
	AI888563	Smoothelin	Cell shape control	2.1	7
	U03057	SNL/fascin1	Cell shape control	2.1	7
Signaling	AL022310	TNF SF 4/OX40L	Cell growth control	16.5	6
	U78305	WIP-1	Cell growth control (p53 inducible)	4.8	7
	U07358	MAP 3K 12	MAP kinase signaling	2.1	6
Immune response	U02388	CYP4F2	Leukotriene metabolism	12.0	6
	J00219	INFγ	Growth suppression	8.0	5
Transcription	W47047	P8 protein	Candidate for metastasis	11.0	5
	AA635153	ZNF 79	Transcription factor	5.4	5
	U59913	**SMAD5**	Growth suppression (TGFβ pathway)	3.6	6
	L19871	ATF3	Stress response	3.5	6
	U68019	SMAD3	Growth suppression (TGFβ pathway)	2.4	6
	L29277	STAT 3	Growth control (INFγ pathway)	2.3	7
	M97936	STAT1	Pro-apoptotic (INFγ pathway)	2.2	6
Cell growth	AB00584	MIC-1	Growth suppression (p53 inducible)	10.9	7
	X16354	**CEACAM1**	Growth suppression	9.3	6
	M14083	PAI-1	Induction of senescence	5.6	6
	AF059611	**NRP/B (Pig10)**	Neurogenesis (p53 inducible)	4.8	7
	AF038844	DUSP14/MPK6	MAPK inactivation	4.7	7
	U72649	**BTG 2**	Growth suppression (p53 inducible)	4.0	7
	AF050110	**TIEG**	Growth suppression (TGFβ pathway, p53 ind)	3.9	7
	U91512	ninjurin1	Neurogenesis	3.8	7
	X61123	BTG1	Growth suppression	2.9	7
	U66469	**CGR19**	Growth suppression (p53 inducible)	2.1	6
	U51127	IRF5	Growth control (INFγ pathway)	1.9	7
Cell cycle	U33203	mdm2 (isoforms D,E,A)	P53 nuclear export (p53 inducible)	5.6	6
	U57317	P/CAF	Acetylation (p53 activation)	4.7	4
	M60974	**GADD45**	Cell cycle arrest (p53 inducible)	3.9	7
	U03106	**p21/Waf1**	Cell cycle arrest (p53 inducible)	3.9	7
	X57348	14-3-3σ	Cell cycle arrest (p53 inducible)	2.8	7
	U83981	GADD34	Cell cycle arrest	2.7	6
	U77949	CDC6	Cell cycle control	2.1	7
	M92287	Cyclin D3	G1/S cyclin	1.8	7
Apoptosis	AF010309	Pig3	Apoptosis induction (p53 inducible)	10.5	7
	U82987	PUMA	Apoptosis induction (p53 inducible)	2.8	7
	U19599	BAX δ	Apoptosis induction (p53 inducible)	2.2	7
	X63717/Z70519	**FAS/APO1**	Apoptosis induction (death receptor)	2.2	7
	L05072	IRF1	Apoptosis induction (INFγ pathway)	2.1	7
	U60519	CASP 10 B	Apoptosis induction	2.1	5
	L22473	BAX α	Apoptosis induction (p53 inducible)	2.1	7
	U37518	TNFSF10	Apoptosis induction	2.0	6
	U77845	hTRIP	Apoptosis induction	2.0	6
	U16811	Bak	Apoptosis induction (p53 inducible)	1.9	6
DNA repair	D21089	XP-C	Nucleotide excision repair (p53 inducible)	4.3	7
	U18300	XP-E/DDB2	Nucleotide excision repair (p53 inducible)	4.3	7
	AF034956	RAD 51 L3	Recombination	2.1	5
	M36067	Ligase I	DNA ligation	2.0	7
	X95152	BRCA2 exon2	Recombination	2.0	6
Down-regulated genes					
Cell growth	V00568	c-myc	Growth stimulation	−3.1	7
	U52682	IRF 4	Growth stimulation	−2.7	7
	U96876	Insulin induced gene 1	Growth stimulation	−1.9	7
	X02160	Insulin receptor	Growth stimulation	−1.9	5
Cell cycle	AF023612	DIM1	Essential for mitosis	−2.4	4
	M25753	Cyclin B1 related	G2/M transition	−1.9	7
	U11791	Cyclin H	CDC2 activation	−1.8	7
Protein folding	AI912041	HSP E1	Heat shock protein	−2.3	7
	M59830	HSP70-2	Heat shock protein	−2.3	6
	Y00371	HSC 70	Heat shock protein	−2.1	7
	M11717	HSP 70	Heat shock protein	−2.0	7
Metabolism	S68805	AGAT	Energetic metabolism	−2.4	6
	X66435	HMGCS1	Lipid metabolism	−2.2	6
	D78130	Squalene Epoxidase	Lipid metabolism	−2.1	7
	X60221	ATP5F1	Energetic metabolism	−2.0	5
Translation	M15353	EIF 4E	Protein synthesis	−2.1	6

[a] Derived from LocusLink and SwissProt databases or recent publications in case of incomplete annotations.
[b] Average signal of MNNG-treated TK6 cells *versus* average signal of untreated TK6 cells.
[c] See "Materials and Methods."

293T cells (Fig. 3*D*), we did not observe any induction of its transcriptional targets upon treatment. On the contrary, some p53-inducible genes such as *p21/WAF1*, *BAX*, and *BTG2* were down-regulated. For *p21/WAF1*, this type of regulation was associated with a decrease of the corresponding polypeptide, as confirmed by immunoblot analysis showed in Fig. 3*E*. Finally, in contrast to the lymphoblastoid cells, the cell cycle arrest was not associated with changes in c-myc RNA and protein levels (Fig. 3*E*).

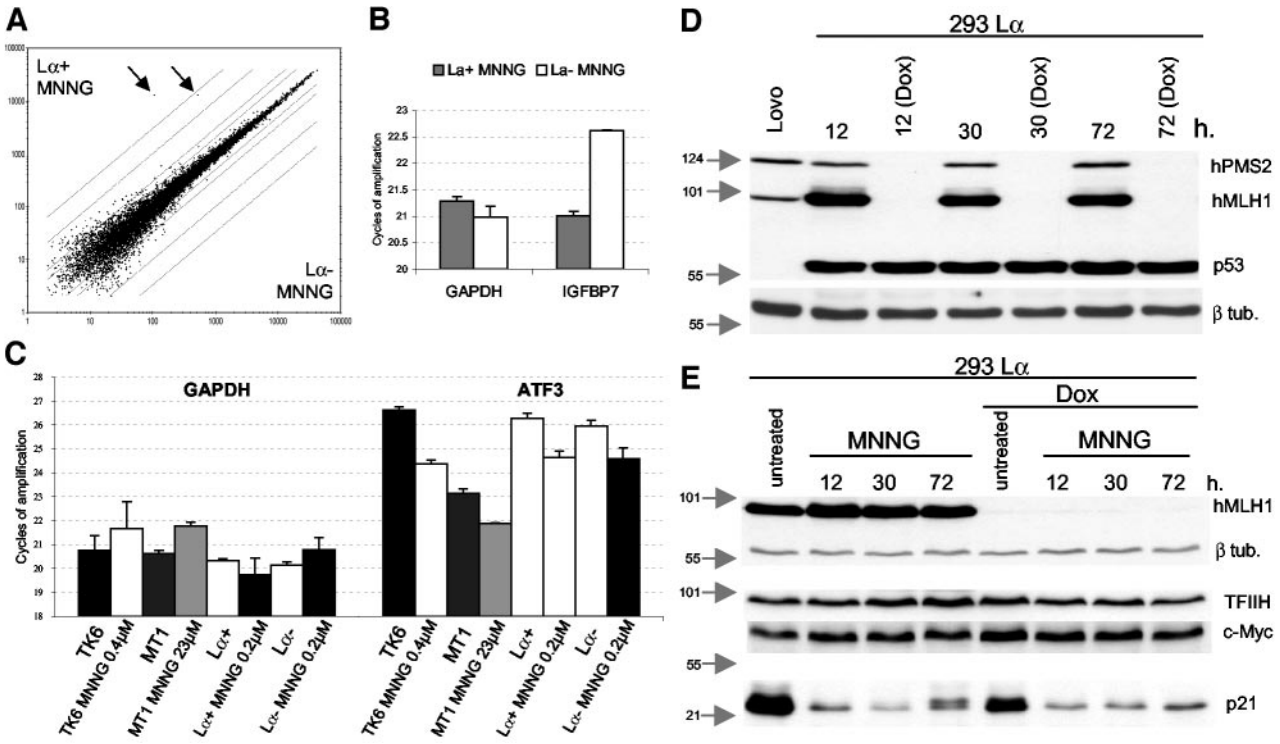

Fig. 3. Microarray data and quantitative evaluation of transcripts and proteins in 293T $L\alpha^+/L\alpha^-$ cells. *A*, several genes were differentially expressed in $L\alpha^+$ cells compared with $L\alpha^-$ 30 h after MNNG treatment (see Table 2 for details). The *arrows* show the two probes for hMLH1. *B*, quantitative RT-PCR analysis of insulin-like growth factor binding protein 7, the 2.6-fold up-regulation of which in $L\alpha^+$ compared with $L\alpha^-$ was confirmed by the difference in TAC (1.5 cycles earlier in $L\alpha+$). GAPDH was used as control. *C*, quantitative RT-PCR analysis of ATF3. Significant increase of this transcript was recorded in all of the cell lines treated with equitoxic amounts of MNNG. *D* and *E*, Western blot analyses showing p53 stabilization (*D*), unchanged c-myc levels and down-regulation of p21 protein levels (*E*). TFIIHp89 and β-tubulin: loading controls. Dox: addition of doxycycline turns off hMLH1 expression.

DISCUSSION

In this work, we investigated the MMR-dependent changes in gene expression occurring upon treatment with the DNA-methylating agent MNNG, using two different human cellular models. Our aim was to mimic what happens in normal and tumor cells exposed to agents that methylate the O^6-position of deoxyguanosine because it is the processing of this lesion by the MMR system that governs the cytotoxicity of these drugs (see "Introduction"). This is the first study in which the global gene expression in human cells treated with methylating agents has been investigated. Similar studies were performed in yeast but using methyl methanesulfonate, which does not methylate on O^6-deoxyguanosine (23, 24). In addition, there is no evidence that the toxicity of methylating agents in yeast is affected by the MMR status (6).

MNNG efficiently killed the MMR-proficient lymphoblastoid TK6 cells in which a cell cycle delay in S phase was followed by apoptosis. This phenomenon could be ascribed to the attempts of the MMR system to process O^6-meG/T mismatches during DNA replication (see "Introduction"). The same repair process is probably responsible for the dramatic transcriptional response leading to cell death. In contrast, MNNG failed to cause even mild perturbation of the cell cycle in the hMSH6-deficient MT1 cells. Microarray experiments showed that the transcriptome of MT1 cells was globally unmodified, whereas in TK6 cells, the treatment had a large impact on gene expression. The presence of many p53-inducible genes and TGF-β effectors among the most up-regulated transcripts in TK6 cells indicates that these two pathways are both activated to arrest cell proliferation. Our data are consistent with a previous microarray experiment in which p53-regulated genes were identified using a human lung cancer cell line expressing temperature-sensitive p53 (25). We detected up-regulation of five DNA repair genes upon MNNG treatment, at least two, XP-C and DDB2, known to carry p53-responsive elements in their promoters (26, 27). Our microarray data revealed that the activation of apoptosis was only partially accomplished through p53-inducible effectors (PIG3, BAX, and PUMA; Refs. 28–31). The up-regulation of IFN-γ and its downstream effectors signal transducers and activators of transcription 1 and IRF1, as well as the induction of Fas/APO1 and some members of the tumor necrosis factor superfamily, suggest also an activation of a proapoptotic cross-talk among cells through the death receptor system (32–34). Surprisingly, the negative modulator of cell cycle p21/WAF1, although transcriptionally activated at 30 h, was not up-regulated at the protein level at this time, when cells were delayed in S phase. That p21/WAF1 is dispensable for cell cycle arrest in this cell cycle phase has already been suggested by the observation that a transient intra-S-phase checkpoint can be p21/WAF1 independent (35). Thus, the fact that the protein level of p21/WAF1 was not changed 30 h after treatment despite an increase in its RNA suggests that a posttranscriptional mechanism may control this function at this time point to promote DNA repair (36) and eventually allow apoptosis (37, 38).

Interesting findings regarding the role of p53 in lymphoblastoid cells treated with low doses of MNNG were gathered when we examined the p53-mutated WTK1 cell line. Microarray analysis (Table 1, genes in bold and Table C, supplementary material) revealed up-regulation of death receptors (Fas/APO1 and TNFRSF 9 and 17) and activation of the TGF-β-dependent signaling through up-regulation of SMAD5 and TIEG (18). Surprisingly, the transcripts of some cell cycle inhibitors such as p21/WAF1, GADD45, CGR19, and BTG2, generally thought to be p53-dependent, were up-regulated to the same extent as in TK6, pointing to a transcriptional activation

Table 2 *Genes*

A. Genes whose expression significantly varied upon MNNG treatment in 293T Lα+ cells compared with Lα− at the time point indicated

	GeneBank access no.	Title	Category[a]	Function[a]	Time point(s)[b]
$L\alpha^+ > L\alpha^-$	L19182	IGFBP7	Signal transduction	Growth suppression	72
	AF059617	SNK	Signal transduction	Mitogenic response	72
	HG3075-HT3236	FAK	Signal transduction	Integrin signaling	72
	HG3484-HT3678	CLK1	Signal transduction	Dual specificity kinase	72
	L06797	CXCR4	Signal transduction	Chemokine receptor (Immune response)	72
	HG2167-HT2237	PK HT31	Signal transduction	Scaffolding for PKA	72
	U19487	PTGER2	Signal transduction	Prostaglandin E2 receptor EP2	72
	U97669	Notch homolog 3	Signal transduction	Cell differentiation	72
	AB022718	DEPP	?	Decidual protein induced by progesterone	72
	U59632	PNUTL1	Cytoskeleton	Cell shape	72
	AB002323	DNCH1	Cytoskeleton	Spindle formation	72
	U66689	ABCC6	Membrane fraction	Small molecule transport	72
	X54871	RAB5B	Membrane fraction	Vesicle transport	72
	M86917	OSBP	Lipid metabolism	Oxysterol binding protein	12
$L\alpha^+ < L\alpha^-$	Y00067	NEF 3	Cytoskeleton	Intermediate filament	72
	W28588	NEFL	Cytoskeleton	Neurofilament	12
	AB007892	CDC5-like	Cell cycle	Spliceosome, G2/M transition	72
	M27396	ASNS	Metabolism	Asparagine synthetase	72
	AB002345	PER2	Metabolism	Not known	30
	U31875	DHRS2	Energetic metabolism	Alcohol dehydrogenase	30, 72
	X03473	H1F0	Nucleosome	Histone	72
	AL049223	SCAMP1	Membrane trafficking	Endocytosis	72
	AB011141	SMADIP1	Transcription	SMAD interacting protein	12
	U79273	clone23933	?	Homology to Alu sequence and EIF4A	72

B. A selection of genes that were up- or down-regulated in 293T Lα cells upon MNNG treatment independently of the hMLH1 expression (for a complete list, see Table D of supplementary material)

	GeneBank	Title	Category[a]	Function[a]	Time point(s)[c]
Up-regulated	V01512	c-fos	Signal transduction	Growth and apoptosis control	12,30,72
	J04111	c-jun	Signal transduction	Growth and apoptosis control	72
	U27193	DUSP8	Signal transduction	JNK-p38 inactivation	12,30,72
	X68277	DUSP1	Signal transduction	JNK inactivation	12,30,72
	AJ131693	AKAP9	Signal transduction	Scaffolding for PKA	72
	J03358	FER	Signal transduction	Kinase	72
	AA224832	STK39 (SPAK)	Signal transduction	Stress response	12
	U83981	GADD34	Cell cycle	Cell growth and apoptosis	30, 72
	L19871	ATF3	Transcription	Stress response	12,30,72
	U66619	SMARCD3	Transcription	Chromatin modeling	12,30,72
	AB007931	Rb-assoc factor 600	Transcription	Zinc finger protein	12,30,72
	S78296	INA	Cytoskeleton	Intermediate filament	12,30,72
	M13452	lamin A	Cytoskeleton	Cell shape	12,30,72
	AA669799	ASMTL	Metabolism	Acetylserotonin methyltransferase-like	12,30,72
	D13642	SF3b	RNA binding prot	Splicing factor	12,30,72
	D64108	DMC1	DNA repair	Recombination	30, 72
Down-regulated	U59305	PK428	Signal transduction	Ser/Thr kinase	12,30,72
	U50062	RIPK1	Signal transduction	Ser/Thr kinase	12,30,72
	M34181	PKA catalytic sub □	Signal transduction	Kinase activity	12, 30
	D88532	PI3K reg sub 3PIK 3R3	Signal transduction	Insulin pathway	12,30,72
	AF007567	IRS4	Signal transduction	Insulin pathway	12,30,72
	L27560	IGFBP5	Signal transduction	Growth stimulation	12
	Z71929	FGFRec 2	Signal transduction	Growth stimulation	12,30,72
	X76061	Rb-like 2 (p130)	Signal transduction	Growth control	12, 30
	Z11695	MAPK1	Signal transduction	Stress response	12,30,72
	L33881	PKC iota	Signal transduction	Kinase	12, 30
	U24153	PAK2	Signal transduction	Apoptotic signaling	12,30,72
	U03106	p21	Cell cycle	Growth suppression	12,30,72
	AF023158	CDC14B	Cell cycle	M-phase regulator	12,30,72
	L07648	MXI1	Cell cycle	c-myc inhibitor	12, 30
	U72649	BTG2	Cell growth	Growth suppression	12, 30
	L22475	BAX γ	Apoptotic signaling	Apoptosis	12,30,72
	U19599	BAX δ	Apoptotic signaling	Apoptosis	12,30,72
	U65092	MSG1	Transcription	Cbp/p300-interacting factor	30, 72
	AF040963	SMAD4	Transcription	Growth suppression	12,30,72
	M27691	CREB1	Transcription	G-protein signaling	12,30,72
	M88163	SMARCA1	Transcription	Chromatin modeling	12
	X13839	Vascular smooth α actin	Cytoskeleton	Cell shape	12,30,72
	X07834	SOD2	Metabolism	Oxidative stress response	12,30,72
	AA877795	ATP6V1D	Metabolism	ATP synthesis	12,30,72
	NM001098	Aconitase	Metabolism	Energy metabolism	12, 30
	M10905	Fibronectin 1	Extracellular matrix	Cell adhesion	12, 30
	L13210	Mac-2 bind protein	Extracellular matrix	Scavenger receptor	12,30
	M61916	Laminin β 1	Extracellular matrix	Basement membrane protein	12, 30
	M82809	Annexin IV	Membrane fraction	Phospholipase A2 inhibitor	12, 30
	U50410	Glypican3	Membrane fraction	Growth control ?	12, 30
	X59841	PBX3	Development	Transcription factor	12,30,72

[a] Derived from LocusLink and SwissProt databases or recent publications in case of incomplete annotations.

[b] Time point at which the multiple regression analysis showed a statistically significant ($P < 0.05$) interaction between the presence of hMLH1 and the time after treatment.

[c] Time point at which the multiple regression analysis showed a significant ($P < 0.05$) up- or down-regulation of the gene upon MNNG treatment regardless of the presence of hMLH1 (in both 293T $L\alpha^+$ and $L\alpha^-$ cells).

independent of p53. In contrast, the proapoptotic p53-targets BAX, PUMA, and PIG3 were unchanged. These findings suggest that MMR-proficient lymphoblastoid cells can use alternative pathways to trigger cell death independently of the transcriptional activity of p53.

The absence of any transcriptional response in MT1 cells exposed to equimolar (0.4 μM) doses of MNNG could be ascribed to mechanisms other than MMR deficiency. We could exclude resistance mediated by detoxifying enzymes because MGMT and GSH-S-transferases have the same pattern of expression as in TK6. In addition, the integrity of the p53-dependent pathway in MT1 was ascertained upon exposure to equitoxic doses (23 μM) of MNNG. However, from the basal gene expression pattern (Table B, supplementary material), it would appear that MT1 cells have acquired a more transformed phenotype than TK6. Seven tumor antigens (GAGE isoforms and BAGE) were among the most up-regulated transcripts in MT1 compared with TK6, as well as the tumorigenic factor PRKACβ (catalytic subunit of PKA). Different isoforms of the tumor marker CD44, found associated with inhibition of apoptosis and growth advantage (39), were overexpressed, whereas the transcript for the structural protein SNL/fascin1, reported to play an important role in cell adhesion and migration of peripheral blood cells (40), was >40 times less abundant. Finally, the balance between proapoptotic and antiapoptotic factors was strongly biased in favor of the latter (see "Results"). Because these findings demonstrated that TK6 and MT1 cells cannot be considered isogenic as previously invoked, we extended our study to the truly isogenic model 293T Lα^+/Lα^-.

As shown for the lymphoblastoid cell lines, only 293T cells with a functional MMR system were sensitive to MNNG, although the features of the cellular response of 293T Lα^+ differed from TK6 in that a G_2-M checkpoint was activated after a transient S-phase slowdown and cell death was delayed. The absence of any sign of apoptosis (upon MNNG and Fas ligand treatments) might be explained by the general tolerance of this cell line to apoptotic stimuli. This phenotype results, at least in part, from the expression of adenovirus E1A and E1B proteins and of SV40 large T antigen (12) that brings about inactivation of p53- (41, 42) and of TGF-β-dependent pathways (43). Indeed, none of the effectors of p53 and TGF-β pathways were transcriptionally induced upon MNNG treatment and some such as the growth inhibitors p21/WAF1, BTG2, and SMAD4, as well as the proapoptotic BAX, were down-regulated. Interestingly, this type of regulation was detected also in the absence of MMR, presumably as a global response of the 293T Lα aimed at surviving the treatment. This is also supported by the enhanced transcription in both 293T Lα^+ and Lα^- of the oncogenes c-fos and c-jun. Among the cellular processes regulated by *c-Fos* and *c-Jun*, a stimulation of cell cycle progression via repression of *p21/WAF1* transcription has been reported (44). A synergistic effect might be accomplished by the up-regulation of the mitogen-activated protein kinase phosphatases DUSP1 and DUSP 8 (Table 2), which have been shown to be involved in the dephosphorylation and inactivation of the stress-inducible and antiproliferative mitogen-activated protein kinases c-Jun NH_2-terminal kinase and p38 (45, 46). This type of gene regulation may suggest that 293T Lα cells sensed the treatment also in the absence of functional MMR. This is additionally witnessed by the up-regulation, independently of the MMR-status, of the transcription factor ATF3, previously correlated with the response to genotoxic agents in a p53-dependent and -independent fashion (22).

These findings suggest that MNNG induces a general response in 293T Lα characterized by an increase of survival signals. Notwithstanding this, 293T Lα^+ cells, where the O^6-meG/T mismatches can be addressed by the MMR, stopped cycling, and eventually died. Indeed, in these cells we detected posttranslational modifications that accompanied the G_2-M arrest (*i.e.,* CHK1 and CHK2 phosphorylation, CDC25A degradation, and CDC2 Tyr^{15} phosphorylation[4]), but in contrast to lymphoblastoid cells, activation of the G_2-M checkpoint was reflected in only a moderate transcriptional response. This might be ascribed to the inactivation of pRb by the transfected E1A that brings about deregulation of E2F activity, a pivotal transcription factor acting in response to cell cycle modulators (47). Microarray data failed to help us identify the pathways responsible of cell death in these cells, yet some signaling molecules, differentially transcribed in MMR-proficient 293T Lα cells upon treatment, might be biologically relevant in determining their cellular fate. One example is the up-regulation of the tumor suppressor insulin-like growth factor binding protein 7/Mac25 that was reported to be down-regulated in some breast cancer cells (21) and increased in cells committed to death by senescence or apoptosis (48, 49). Taken together, these data showed that although MNNG can induce a general stress response in 293T Lα cells, its cytotoxicity depends exclusively on the recognition and processing of DNA damage by the MMR system. The absence of MGMT in these cells, as well as in TK6 cells, enabled us to use doses of MNNG that were so low as to prevent any MMR-independent cytotoxicity.

In conclusion, we demonstrated that in the presence of DNA methylation damage, the MMR system swings the balance between survival and death in favor of the latter. The type of response strongly depends on the cellular background and relies on the signaling pathways available to the cells. Although p53 may be one of the main effectors of cell death induced by MNNG, its inactivation does not prevent cell death. The experiments with 293T cells showed that even in the presence of strong survival signals, a situation that might mimic tumor environment, MMR is sufficient to activate pathways leading to proliferation arrest and eventually cell death. Thus, MMR most likely plays a crucial role in the efficacy of methylating agents in cancer therapy. Unfortunately, by playing a similar role also in rapidly proliferating normal tissues such as bone marrow and gastrointestinal mucosa, MMR is responsible for the toxicity of this treatment. To prevent side effects, lower doses of methylating agents would have to be deployed, which requires that the level of MGMT in the tumor be reduced. Targeted down-regulation of this enzyme in MMR- and MGMT-positive tumors is subject to investigation.

ACKNOWLEDGMENTS

We thank Christine Hemmerle for technical assistance and for help with flow cytometry and Stefano Ferrari and Phaik Morgenthaler for critical comments. We also thank the group of bioinformaticians and technicians of the Functional Genomics Center Zurich for their help and advice.

REFERENCES

1. Karran, P., and Bignami, M. Drug-related killings: a case of mistaken identity. Chem. Biol., *3:* 875–879, 1996.
2. Branch, P., Aquilina, G., Bignami, M., and Karran, P. Defective mismatch binding and a mutator phenotype in cells tolerant to DNA damage. Nature (Lond.), *362:* 652–654, 1993.
3. Kat, A., Thilly, W. G., Fang, W. H., Longley, M. J., Li, G. M., and Modrich, P. An alkylation-tolerant, mutator human cell line is deficient in strand-specific mismatch repair. Proc. Natl. Acad. Sci. USA, *90:* 6424–6428, 1993.
4. Koi, M., Umar, A., Chauhan, D. P., Cherian, S. P., Carethers, J. M., Kunkel, T. A., and Boland, C. R. Human chromosome 3 corrects mismatch repair deficiency and microsatellite instability and reduces *N*-methyl-*N*′-nitro-*N*-nitrosoguanidine tolerance in colon tumor cells with homozygous hMLH1 mutation. Cancer Res., *54:* 4308–4312, 1994.
5. Hawn, M. T., Umar, A., Carethers, J. M., Marra, G., Kunkel, T. A., Boland, C. R., and Koi, M. Evidence for a connection between the mismatch repair system and the G_2 cell cycle checkpoint. Cancer Res., *55:* 3721–3725, 1995.

[4] L. Stojic, N. Mojas, P. Cejka, M. di Pietro, S. Ferrari, G. Marra, and J. Jiricny. DNA damage signalling induced by S_N1 type methylating agents and its dependence on a functional mismatch repair system, manuscript in preparation.

6. Marra, G., and Schaer, P. Recognition of DNA alterations by the mismatch repair system. Biochem. J., *338:* 1–13, 1999.
7. Cejka, P., Stojic, L., Mojas, N., Russell, A. M., Heinimann, K., Cannavo, E., di Pietro, M., Marra, G., and Jiricny, J. Methylation-induced G_2-M arrest requires a full complement of the mismatch repair protein hMLH1. EMBO J., *22:* 2245–2254, 2003.
8. Jass, J. R., Whitehall, V. L., Young, J., and Leggett, B. A. Emerging concepts in colorectal neoplasia. Gastroenterology, *123:* 862–876, 2002.
9. D'Atri, S., Tentori, L., Lacal, P. M., Graziani, G., Pagani, E., Benincasa, E., Zambruno, G., Bonmassar, E., and Jiricny, J. Involvement of the mismatch repair system in temozolomide-induced apoptosis. Mol. Pharmacol., *54:* 334–341, 1998.
10. Hickman, M. J., and Samson, L. D. Role of DNA mismatch repair and p53 in signaling induction of apoptosis by alkylating agents. Proc. Natl. Acad. Sci. USA, *96:* 10764–10769, 1999.
11. Duckett, D. R., Bronstein, S. M., Taya, Y., and Modrich, P. hMutSα- and hMutLα-dependent phosphorylation of p53 in response to DNA methylator damage. Proc. Natl. Acad. Sci. USA, *96:* 12384–12388, 1999.
12. DuBridge, R. B., Tang, P., Hsia, H. C., Leong, P. M., Miller, J. H., and Calos, M. P. Analysis of mutation in human cells by using an Epstein-Barr virus shuttle system. Mol. Cell. Biol., *7:* 379–387, 1987.
13. Trojan, J., Zeuzem, S., Randolph, A., Hemmerle, C., Brieger, A., Raedle, J., Plotz, G., Jiricny, J., and Marra, G. Functional analysis of hMLH1 variants and HNPCC-related mutations using a human expression system. Gastroenterology, *122:* 211–219, 2002.
14. Goldmacher, V. S., Cuzick, R. A. J., and Thilly, W. G. Isolation and partial characterization of human cell mutants differing in sensitivity to killing and mutation by methylnitrosourea and *N*-methyl-*N′*-nitro-*N*-nitrosoguanidine. J. Biol. Chem., *261:* 12462–12471, 1986.
15. Papadopoulos, N., Nicolaides, N. C., Liu, B., Parsons, R., Lengauer, C., Palombo, F., D'Arrigo, A., Markowitz, S., Willson, J. K., Kinzler, K. W., and Vogelstein, B. Mutations of GTBP in genetically unstable cells. Science (Wash. DC), *268:* 1915–1917, 1995.
16. Xia, F., Wang, X., Wang, Y. H., Tsang, N. M., Yandell, D. W., Kelsey, K. T., and Liber, H. L. Altered p53 status correlates with differences in sensitivity to radiation-induced mutation and apoptosis in two closely related human lymphoblast lines. Cancer Res., *55:* 12–15, 1995.
17. Pelengaris, S., Khan, M., and Evan, G. c-MYC: more than just a matter of life and death. Nat. Rev. Cancer, *2:* 764–776, 2002.
18. Ten Dijke, P., Goumans, M. J., Itoh, F., and Itoh, S. Regulation of cell proliferation by Smad proteins. J. Cell. Physiol., *191:* 1–16, 2002.
19. Beere, H. M., and Green, D. R. Stress management: heat shock protein-70 and the regulation of apoptosis. Trends Cell Biol., *11:* 6–10, 2001.
20. Okuyama, T., Ishihara, S., Sato, H., Rumi, M. A., Kawashima, K., Miyaoka, Y., Suetsugu, H., Kazumori, H., Cava, C. F., Kadowaki, Y., Fukuda, R., and Kinoshita, Y. Activation of prostaglandin E2-receptor EP2 and EP4 pathways induces growth inhibition in human gastric carcinoma cell lines. J. Lab. Clin. Med., *140:* 92–102, 2002.
21. Landberg, G., Ostlund, H., Nielsen, N. H., Roos, G., Emdin, S., Burger, A. M., and Seth, A. Down-regulation of the potential suppressor gene IGFBP-rP1 in human breast cancer is associated with inactivation of the retinoblastoma protein, cyclin E overexpression and increased proliferation in estrogen receptor negative tumors. Oncogene, *20:* 3497–3505, 2001.
22. Fan, F., Jin, S., Amundson, S. A., Tong, T., Fan, W., Zhao, H., Zhu, X., Mazzacurati, L., Li, X., Petrik, K. L., Fornace, A. J., Jr., Rajasekaran, B., and Zhan, Q. ATF3 induction following DNA damage is regulated by distinct signaling pathways and overexpression of ATF3 protein suppresses cells growth. Oncogene, *21:* 7488–7496, 2002.
23. Jelinsky, S. A., and Samson, L. D. Global response of *Saccharomyces cerevisiae* to an alkylating agent. Proc. Natl. Acad. Sci. USA, *96:* 1486–1491, 1999.
24. Chen, D., Toone, W. M., Mata, J., Lyne, R., Burns, G., Kivinen, K., Brazma, A., Jones, N., and Bahler, J. Global transcriptional responses of fission yeast to environmental stress. Mol. Biol. Cell, *14:* 214–229, 2003.
25. Kannan, K., Amariglio, N., Rechavi, G., Jakob-Hirsch, J., Kela, I., Kaminski, N., Getz, G., Domany, E., and Givol, D. DNA microarrays identification of primary and secondary target genes regulated by p53. Oncogene, *20:* 2225–2234, 2001.
26. Adimoolam, S., and Ford, J. M. p53 and DNA damage-inducible expression of the xeroderma pigmentosum group C gene. Proc. Natl. Acad. Sci. USA, *99:* 12985–12990, 2002.
27. Hwang, B. J., Ford, J. M., Hanawalt, P. C., and Chu, G. Expression of the *p48 xeroderma pigmentosum* gene is p53-dependent and is involved in global genomic repair. Proc. Natl. Acad. Sci. USA, *96:* 424–428, 1999.
28. Polyak, K., Xia, Y., Zweier, J. L., Kinzler, K. W., and Vogelstein, B. A model for p53-induced apoptosis. Nature (Lond.), *389:* 300–305, 1997.
29. Vousden, K. H., and Lu, X. Live or let die: the cell's response to p53. Nat. Rev. Cancer, *2:* 594–604, 2002.
30. Nakano, K., and Vousden, K. H. PUMA, a novel proapoptotic gene, is induced by p53. Mol. Cell., *7:* 683–694, 2001.
31. Yu, J., Wang, Z., Kinzler, K. W., Vogelstein, B., and Zhang, L. PUMA mediates the apoptotic response to p53 in colorectal cancer cells. Proc. Natl. Acad. Sci. USA, *100:* 1931–1936, 2003.
32. Fulda, S., and Debatin, K. M. IFN-γ sensitizes for apoptosis by up-regulating caspase-8 expression through the Stat1 pathway. Oncogene, *21:* 2295–2308, 2002.
33. Guzman-Rojas, L., Sims-Mourtada, J. C., Rangel, R., and Martinez-Valdez, H. Life and death within germinal centres: a double-edged sword. Immunology, *107:* 167–175, 2002.
34. Ashkenazi, A. Targeting death and decoy receptors of the tumour-necrosis factor superfamily. Nat. Rev. Cancer, *2:* 420–430, 2002.
35. Bartek, J., and Lukas, J. Mammalian G_1- and S-phase checkpoints in response to DNA damage. Curr. Opin. Cell Biol., *13:* 738–747, 2001.
36. Bendjennat, M., Boulaire, J., Jascur, T., Brickner, H., Barbier, V., Sarasin, A., Fotedar, A., and Fotedar, R. UV irradiation triggers ubiquitin-dependent degradation of p21/WAF1 to promote DNA repair. Cell, *114:* 599–610, 2003.
37. Javelaud, D., and Besancon, F. Inactivation of p21WAF1 sensitizes cells to apoptosis via an increase of both p14ARF and p53 levels and an alteration of the Bax/Bcl-2 ratio. J. Biol. Chem., *277:* 37949–37954, 2002.
38. Zhang, Y., Fujita, N., and Tsuruo, T. Caspase-mediated cleavage of p21Waf1/Cip1 converts cancer cells from growth arrest to undergoing apoptosis. Oncogene, *18:* 1131–1138, 1999.
39. Naot, D., Sionov, R. V., and Ish-Shalom, D. CD44: structure, function, and association with the malignant process. Adv. Cancer Res., *71:* 241–319, 1997.
40. Kureishy, N., Sapountzi, V., Prag, S., Anilkumar, N., and Adams, J. C. Fascins, and their roles in cell structure and function. Bioessays, *24:* 350–361, 2002.
41. Steegenga, W. T., van Laar, T., Riteco, N., Mandarino, A., Shvarts, A., van der Eb, A. J., and Jochemsen, A. G. Adenovirus E1A proteins inhibit activation of transcription by p53. Mol. Cell. Biol., *16:* 2101–2109, 1996.
42. Pipas, J. M., and Levine, A. J. Role of T antigen interactions with p53 in tumorigenesis. Semin. Cancer Biol., *11:* 23–30, 2001.
43. Nishihara, A., Hanai, J., Imamura, T., Miyazono, K., and Kawabata, M. E1A inhibits transforming growth factor-β signaling through binding to Smad proteins. J. Biol. Chem., *274:* 28716–28723, 1999.
44. Shaulian, E., and Karin, M. AP-1 as a regulator of cell life and death. Nat. Cell Biol., *4:* E131–E136, 2002.
45. Sanchez-Perez, I., Martinez-Gomariz, M., Williams, D., Keyse, S. M., and Perona, R. CL100/MKP-1 modulates JNK activation and apoptosis in response to cisplatin. Oncogene, *19:* 5142–5152, 2000.
46. Chen, Y. R., Shrivastava, A., and Tan, T. H. Down-regulation of the c-Jun N-terminal kinase (JNK) phosphatase M3/6 and activation of JNK by hydrogen peroxide and pyrrolidine dithiocarbamate. Oncogene, *20:* 367–374, 2001.
47. Classon, M., and Harlow, E. The retinoblastoma tumour suppressor in development and cancer. Nat. Rev. Cancer, *2:* 910–917, 2002.
48. Lopez-Bermejo, A., Buckway, C. K., Devi, G. R., Hwa, V., Plymate, S. R., Oh, Y., and Rosenfeld, R. G. Characterization of insulin-like growth factor-binding protein-related proteins (IGFBP-rPs) 1, 2, and 3 in human prostate epithelial cells: potential roles for IGFBP-rP1 and 2 in senescence of the prostatic epithelium. Endocrinology, *141:* 4072–4080, 2000.
49. Sprenger, C. C., Vail, M. E., Evans, K., Simurdak, J., and Plymate, S. R. Overexpression of insulin-like growth factor binding protein-related protein-1(IGFBP-rP1/mac25) in the M12 prostate cancer cell line alters tumor growth by a delay in G_1 and cyclin A associated apoptosis. Oncogene, *21:* 140–147, 2002.